BRAIN
ORIGINAL ARTICLE

Alzheimer proteopathic tau seeds are biochemically a *forme fruste* of mature paired helical filaments

Mukesh Kumar,[1,2,†,‡] Noé Quittot,[1,3,†] Simon Dujardin,[1,3,§] Christoph N. Schlaffner,[1,2,#,††] Arthur Viode,[1,4] Anne Wiedmer,[3] Pieter Beerepoot,[1,2] Joshua E. Chun,[1,3] Calina Glynn,[1,3] Analiese R. Fernandes,[3] Cameron Donahue,[3] Judith A. Steen[1,2] and Bradley T. Hyman[1,3]

[†]These authors contributed equally to this work

Aggregation prone molecules, such as tau, form both historically well characterized fibrillar deposits (neurofibrillary tangles) and recently identified phosphate-buffered saline (PBS) extract species called proteopathic seeds. Both can cause normal endogenous tau to undergo templated misfolding. The relationship of these seeds to the fibrils that define tau-related diseases is unknown. We characterized the aqueous extractable and sarkosyl insoluble fibrillar tau species derived from human Alzheimer brain using mass spectrometry and *in vitro* bioassays. Post-translational modifications (PTMs) including phosphorylation, acetylation and ubiquitination are identified in both preparations. PBS extract seed competent tau can be distinguished from sarkosyl insoluble tau by the presence of overlapping, but less abundant, PTMs and an absence of some PTMs unique to the latter. The presence of ubiquitin and other PTMs on the PBS-extracted tau species correlates with the amount of tau in the seed competent size exclusion fractions, with the bioactivity and with the aggressiveness of clinical disease. These results demonstrate that the PTMs present on bioactive, seed competent PBS extract tau species are closely related to, but distinct from, the PTMs of mature paired helical filaments, consistent with the idea that they are a *forme fruste* of tau species that ultimately form fibrils.

1 Department of Neurology, Harvard Medical School, Boston, MA 02115, USA
2 F.M. Kirby Neurobiology Center, Boston Children's Hospital, Boston, MA 02115, USA
3 Alzheimer Research Unit, Department of Neurology, Massachusetts General Hospital, Boston, MA 02129, USA
4 Department of Pathology, Boston Children's Hospital, Boston, MA 02115, USA
‡ Present address: Cell Signaling Technology, Inc., Danvers, MA 01923, USA
§ Present address: Sanofi, Cambridge, MA 02139, USA
# Present address: Data Analytics and Computational Statistics, Hasso Plattner Institute for Digital Engineering, 14482 Potsdam, BB, Germany
†† Present address: Digital Engineering Faculty, University of Potsdam, 14482 Potsdam, BB, Germany

Correspondence to: Bradley T. Hyman
Massachusetts General Hospital/Harvard Medical School
114 16th street, Charlestown, MA 02129, USA
E-mail: bhyman@mgh.harvard.edu

Received January 23, 2023. Revised September 22, 2023. Accepted October 10, 2023. Advance access publication January 18, 2024

Correspondence may also be addressed to: Judith Steen Boston
Children's Hospital/Harvard Medical School
Boston, MA 02115, USA
E-mail: Judith.Steen@childrens.harvard.edu

Keywords: PTM; mass spectrometry; proteomics; neurodegeneration; human Alzheimer disease; Tau protein

Introduction

Tau protein fibrillar aggregates are neuropathological hallmarks of neurodegenerative diseases known as tauopathies.[1] Major structural alterations in tau conformation underlie the mechanisms of tau fibrillar assembly.[2,3] Tau fibrils exist with distinct structural and biochemical characteristics across different tauopathies, as exemplified by classical electron microscopy and more recent cryogenic electron microscopy (cryo-EM) studies.[4-9] This variety of tau conformations is likely at the basis of major differences in the anatomical and clinical progression of the pathology and differences in clinical presentations of the tauopathies.[10,11] However, despite extensive study, including cryo-EM defined structural analyses, the early steps of tau misfolding that subserve aggregation prone species are unknown.

In contrast with the well defined and classically characterized end stage fibrillar species, recent focus has come on the characteristics of aqueous buffer extracts, seeding competent oligomeric tau species that appear to be critical for the propagation of tau conformational information between cells and across neural systems.[12-16] Maeda *et al.*[17] described a 40mer tau oligomer having granular structures and a mild cognitive impairment (MCI) epitope, indicating that this granular tau oligomer consists of conformationally changed tau. The size of granular tau oligomer ranges from 5 to 50 nm.[18] Sahara *et al.*[19] reported the presence of granular aggregates and short filaments in 6-month-old rTg4510 mice. These tau species thus appear to be key for tau proteopathic seeding.[10,15,16,20,21] However, the specific post-translational modifications (PTMs) of these proteopathic seeds from phosphate-buffered saline (PBS) extracts, and how (or if) these species are related to mature fibrils, is largely a matter of speculation. To date, the PBS-extracted seed competent species have only been characterized by their properties on size exclusion chromatography, by atomic force microscopy[15] and by the presence of multiple (highly variable) phosphor-epitopes largely overlapping with fibrillar tau deposits.[15,22] In the current study, we define the biochemical and pathophysiological properties of the different preparations of tau defined operationally as (i) PBS buffer extract, seeding competent, high molecular weight (HMW) tau species (hereafter referred as HMW tau); compared to (ii) sarkosyl insoluble, tau species [hereafter referred as paired helical filaments (PHF) tau]. This comparison aims to explore the hypothesis that the HMW tau species are potential precursors to PHF, and to explore the alternate possibility that HMW species are simply fragments of PHFs, consequent to homogenization and isolation procedures. Using a combination of mass spectrometry (MS)-based proteomics[23,24] and biological characterization, we describe the PTMs of seeding-competent HMW tau from the brains of patients with Alzheimer's disease, compared to seeding competent PHF tau derived from the same patients. We confirm both heterogeneity among samples as well as key molecular links between the proteopathic HMW tau seeds and mature fibrillar PHF tau. While highly similar overall, there are fundamental differences in the numbers and, in a minority of instances, the exact locations of modifications such as phosphorylation, ubiquitination and acetylation observed between HMW and PHF tau. We further examined the clinical importance of these newly described signatures of HMW tau and demonstrate strong correlations of PTMs of tau, especially ubiquitinylation, with tau seeding bioactivity and, importantly, with clinical rates of progression. The identification of these modifications will help us to understand the biology that underlies tau propagation, clinical progression and potentially early stages of neurofibrillary tangle (NFT) formation in Alzheimer's disease.

Material and methods

Human tissue and data collection

Seven human participants with Alzheimer's disease and three control subjects were selected from the Massachusetts Alzheimer's Disease Research Center Longitudinal Cohort study on the basis of the following criteria: (i) clinically diagnosed with dementia due to probable Alzheimer's disease; (ii) cognitive status assessed at least three times by a neurologist at the MGH Memory Clinic Unit and scored using Clinical Dementia Rating Scale Sum of Boxes (CDR-SOB); (iii) diagnosis of Alzheimer's disease confirmed post-mortem by a Massachusetts General Hospital neuropathologist; (iv) Braak NFTs stage V or VI as determined by the location of NFTs with a total tau immunostaining and Bielchowsky's silver stain[25-27]; and (v) the least possible concurrent pathologies. Along with Braak stage, age at death, post-mortem interval and sex were also collected and are listed in Supplementary Table 1.[28] Autopsy tissue from human brains were collected at Massachusetts General Hospital, with informed consent and approval of local institutional review boards.

Human brains were processed as previously described.[3] Briefly, all brains were separated into two hemispheres, one of which was initially sliced coronally at the time of autopsy and 1-cm thick slabs were immediately flash frozen and stored at –80°C. Approximately 2 g of frontal cortex was dissected out of the frozen brain section corresponding to Brodmann area 8/9 and kept at –80°C until homogenization.

Tissue homogenization

Frozen human tissue (1 g) was thawed on wet ice, grey matter dissected and then immediately homogenized in 5 ml of PBS + protease inhibitor (Roche) + Trichostatin A (Sigma) in a 2-ml glass Dounce homogenizer. Tissue was Dounce homogenized with 30 up-and-down strokes on ice by hand. The homogenate was centrifuged at 10 000*g* for 10 min at 4°C. The supernatant was collected and aliquoted to avoid excessive freeze–thaw cycles. A BCA assay (Thermo Scientific Pierce) was performed to determine total protein concentration, and a total tau ELISA (Meso Scale Diagnostics) was performed to determine the concentration of total tau in the samples, following the manufacturer's protocol.

Preparation of oligomeric high molecular weight tau seeds

Brain extracts were separated by size exclusion chromatography (SEC), as previously described[2] on single Superdex 200 10/300GL

columns (no. 17-5175-01, GE Healthcare) in PBS (Cat. No. P3813, Sigma-Aldrich, filtered through a 0.2-μm membrane filter), at a flow rate of 0.5 ml/min, with an AKTA purifier 10 (GE Healthcare). Each brain extract was diluted with PBS to contain 6000 ng of human tau to a final volume of 500 μl, which was filtered through a 0.2-μm membrane filter and then loaded onto an SEC column. Fractions of 500 μl were retrieved. Fractions 2-3-4 previously described to show high seeding competency[2,3] were pooled and sedimented by ultracentrifugation at 150 000*g* for 50 min at 4°C. Pellets were resuspended in PBS, aliquoted and stored at −80°C until analysis by discovery MS, FLEXITau MS and biosensor seeding assay. For the label-free MS, the PBS extracts inputs of the SEC were sedimented by ultracentrifugation at 150 000*g* for 50 min at 4°C. Pellets were then analysed as previously described.[3]

Preparation of sarkosyl insoluble tau

Approximately 150 mg post-mortem brain tissue was homogenized using Precellys 24 tissue homogenizer (5500 speed, three cycles of 20 s with a pause of 30 s) in 640 μl Tris-buffered saline (TBS) lysis buffer containing cocktail of protease, phosphatase and deacetylase inhibitor. Tissue lysates were centrifuged at 20 000*g* for 20 min at 4°C. The supernatant (S1) was transferred to a new tube. To the pellet, 640 μl of 1× salt sucrose buffer was added. The samples were homogenized as above and sonicated on a Qsonica sonicator (time 30 s, pulse 10 s with 5-s pause and an amplitude of 20%, one round for each sample). The samples were centrifuged as above and the supernatant was transferred into a new tube (S2). To the S1, 640 μl of 2× salt sucrose buffer was added to get the same concentration of salt sucrose buffer in both the S1 and S2 samples. Final sarkosyl (1%) was added to each sample and thermomixed at room temperature for 90 min. Samples was transferred to microfuge polypropylene tubes and ultra-centrifuged at 150 000*g*, for 90 min at 4°C. The supernatant, containing the sarkosyl-soluble proteins, was transferred to a new tube and the pellet containing pathogenic insoluble fibrillar paired helical filament tau was stored at −80°C until further processing.

Semi-denaturing detergent agarose gel electrophoresis

Semi-denaturing detergent agarose gel electrophoresis (SDD-AGE) was performed as previously described.[29,30] Brain extracts were loaded onto a 1% agarose gel with Laemmli buffer (20 mmol/l Tris-base, 200 mmol/l glycine and 0.02% sodium dodecyl sulphate). The gel was run at 4°C at 35 V for 16 h and then transferred onto a polyvinylidene difluoride (PVDF) membrane overnight in TBS using filter paper and capillary action. The membrane was blocked in TBS containing 0.25% Tween 20% and 5% non-fat dry milk and incubated overnight with rabbit polyclonal anti-tau antibody (1:5000; Dako). Horseradish peroxidase-conjugated goat anti-rabbit IgG secondary antibody was applied in blocking solution on Day 2 and was detected using chemiluminescent horseradish-peroxidase substrate (Thermo Fisher Scientific) and film (GE Healthcare Life Sciences).

Ubiquitin immunoprecipitation

Ubiquitin immunoprecipitation was performed using the UBIQAPTURE-Q® kit (Enzo Life Science, Cat. No. BML-UW8995-0001) following the manufacturer's instructions. Briefly, tau seeds were incubated with the affinity matrix at 4°C overnight on a horizontal rotor mixer and then centrifugated at 5000*g*, 4°C for 1 min. Supernatants were collected and run on the seeding biosensor assay. Pellets were washed with PBS, spun again at 5000*g*, 4°C for 1 min. Pellets were analysed by western blotting.

Western blot

NuPAGE LDS sample buffer (4× concentration) (Invitrogen) and 10× NuPAGE sample reducing agent (Invitrogen) were added to 5 μg of tau seeds and ubiquitin-immunodepleted tau seeds, boiled for 10 min at 95°C and run on 4–12% Bis-Tris SDSPAGE (Invitrogen) in MOPS buffer (Invitrogen). The gels were transferred to a nitrocellulose membrane. Blots were incubated with anti-total tau polyclonal (anti-C-terminus tau polyclonal, 1:2000; Dako) or monoclonal (anti-N-terminus tau monoclonal Tau-13, 1:1000; BioLegend) or polyclonal anti-ubiquitin (1:1000; Enzo Life Science, Cat. No. UG9511-0100) antibodies overnight at 4°C. Blots were washed three times for 10 min with TBS-T and incubated with secondary anti-or mouse rabbit IRDye680 or IRDye800 (1:5000) for 1 h at room temperature and imaged on the Odyssey infrared imaging system (Li-Cor).

In vitro tau biosensor seeding assay

The *in vitro* seeding assay has previously been described and widely characterized.[31] Briefly, the Tau RD P301S FRET Biosensor (ATCC CRL-3275) cells stably expressing the repeat domain of tau with the p.P301S mutation conjugated to either cyan fluorescent protein (CFP) or yellow fluorescent protein (YFP) (TauRD-P301S-CFP/YFP) were cultured at 37°C, 5% CO_2 in Dulbecco's modified Eagle medium (DMEM), 10% vol/vol fetal bovine serum (FBS), 0.5% vol/vol penicillin–streptomycin. Cells were plated on Costar Black, clear-bottom 96-well plates (previously coated with 1:20 poly-D-lysine) at a density of 40 000 cells per well. Tau preparations, or immunodepleted extracts (1 μl per well), were then incubated with Lipofectamine 2000 (Invitrogen, final concentration 1% vol/vol) in Opti-MEM (final volume of 50 μl per well) for 20 min at room temperature before being added to the cells. Each condition was applied in triplicate or quadruplicate.

Tau seeding was subsequently analysed using flow cytometry: after 24 h, medium was removed and 50 μl trypsin 1× was added for 7 min at 37°C. Chilled DMEM + 10% FBS (150 μl) was added to the trypsin and cells were transferred to 96-well U-bottom plates (Corning). Cells were pelleted at 500*g*, resuspended in freshly made 2% vol/vol paraformaldehyde in PBS (Electron Microscopy Services) for 10 min at room temperature in the dark, and pelleted at 500*g*. Cells were resuspended in chilled PBS and run on the MACSQuant VYB (Miltenyi) flow cytometer. CFP and FRET were both measured by exciting the cells using the 405-nm laser and reading fluorescence emission at the 405/50-nm and 525/50-nm filters, respectively. To quantify the FRET signal, a bivariate plot of FRET versus the CFP donor was generated and cells that received control brain extract alone were used to identify the FRET-negative population. Using this gate, the tau seeding value for each well was calculated by multiplying the percentage of FRET-positive cells by the median fluorescence intensity of that FRET-positive population. We analysed 40 000 events per well. Data were analysed using the MACSQuantify software (Miltenyi).

Mass spectrometric analysis of seed competent high molecular weight and paired helical filament tau

SEC-purified PBS extracts that ran at HMW and have been shown to contain seed-competent tau material and sarkosyl insoluble

fibrillary matured paired helical filament tau were further processed and analysed by LC-MS/MS [liquid chromatography (LC)-tandem MS]. Total protein concentration was determined by bicinchoninic acid assay (Pierce™ BCA Protein Assay Kit, Thermo Scientific). Approximately 50 µg of total protein sample was digested using the filter-aided sample preparation (FASP) method, as previously described.[32] Briefly, total protein was denatured using 8 M urea, protein disulphide bonds were reduced using 10 mM dithiothreitol (DTT) and cysteines were alkylated using 1% acrylamide. Reduced and alkylated protein mixtures were digested with endoproteinase trypsin (sequencing grade modified trypsin, Promega) overnight at 37°C with protease:protein ratio of 1:25 (w/w). Peptides were eluted first with 50 mM ammonium bicarbonate and finally with 0.5 M sodium chloride (NaCl). Peptide eluates were acidified and desalted using reversed phase C-18 microspin columns (SEMSS18V, Nest Group). Peptides were vacuum-dried and reconstituted in sample buffer [5% formic acid, 5% acetonitrile (ACN)]. Samples were randomized and analysed in duplicates using timsTOF Pro mass spectrometer coupled with ultra-high-pressure nano-flow LC nanoElute system (Bruker). Peptides were loaded on to a reverse phase 25 cm aurora series C18 analytical column (25 cm × 75 µm ID, 1.6 µm C18) fitted with captive spray insert (Ion opticks). Column temperature was maintained at 50°C and mobile phase A (2% acetonitrile and 0.1% formic acid in water) and mobile phase B (0.1% formic acid in acetonitrile) was used for the separation of peptide with 400 nl/min constant flow using a linear gradient starting from 0% to 30% in 90 min, followed by an increase to 80% B within 10 min, followed by washing and re-equilibration for 20 min. Mass spectra was acquired on a hybrid trapped ion mobility spectrometry (TIMS)—quadrupole time of flight (TOF) mass spectrometer (timsTOF Pro) with a modified nano-electrospray CaptiveSparay ion source, (Bruker Daltonics). MS was operated in parallel accumulation seerial fragmentation (PASEF) mode. Full mass spectra were acquired in a mass range of 100–1700 m/z and ion mobility (1/k0) range from 0.60–1.60. Ten PASEF MS/MS scans per topN acquisition cycle were acquired. Acquired mass spectra was processed using Bruker DataAnalysis software, mascot generic files (mgf) were searched against a *Homo sapiens* uniport protein database containing 42 389 entries (downloaded on 14 August 2020), supplemented with common contaminants cRAP protein sequences (116 entries) with ProteinPilot™ Software v5.0.1(Sciex). The following settings were applied: instrument type 'Orbi MS (1–3 ppm)'; 'Orbi MS/MS'; 'Urea denaturation'; 'Cysteine alkylation-Acrylamide'; 'Digestion-Trypsin'; 'thorough' search mode; 'phosphorylation emphasis'; 'ID focus on biological modifications'; 'FDR Analysis-Yes'. Mascot v2.6 (Matrix Science, Ltd) was also used for searching the data, and the following settings were used: type of search-MS/MS Ion Search; enzyme-Trypsin/P; Fixed modifications-Propionamide (C); Variable modifications-Acetyl (K); Ubiquitination- GG (K); Oxidation (M); Phospho (ST); Peptide mass tolerance-±10 ppm; Fragment mass tolerance-±0.05 Da; Max missed cleavages-2; significance threshold $P < 0.05$. Similarity between HMW and PHF tau was assessed for PTMs and FLEXITau using random resampling and cosine similarity with Student *t*-tests, respectively.

FLEXITau analysis of PBS extract size exclusion purified seed competent tau

FLEXITau analysis was performed as previously described.[21] The targeted FLEXITau analysis was carried out using a micro-autosampler AS2 and nanoflow HPLC pump module (Eksigent/Sciex) coupled to a triple quadrupole MS (Sciex Qtrap 5500). The chromatographic separation was performed on a Protecol C18G 200Å, 250 mm × 300 µm ID (Trajan) at a flow rate of 5 µl/min in 25 min. A gradient of solvent A (water + 0.1% formic acid) and B (acetonitrile + 0.1% formic acid) was used for elution. Samples were loaded onto the column and peptides were eluted using 2% solvent B and increased to 10% in 2 min. The gradient was ramped to 35% B in 13 min. Then the percentage of mobile phase B was increased to 90% for 5 min. Finally, the column was re-equilibrated at 2% for the following 5 min. Three to five transitions were monitored for each precursor by SRM with a retention time window of 45 s and a target scan time of 0.5 s to ensure optimal data point per peak. Data were analysed with Skyline-daily (version 20.1.9.234),[33] each paired light and heavy precursors were manually checked for similar ratio among transitions, peak shape and retention time. The peak area ratios of light-to-heavy for each peptide were then exported for further calculations. The modifications extent was calculated after normalization of the peak area ratio to the mean of the three peptides with the highest ratio.

Negative stain microscopy

Three microlitres, containing 0.1 µg of total tau measured by western blot, of each sample was applied to a 200 mesh Cu F/C grid for 2 min and then wicked away. Grids were then washed with 3 µl of deionized water. This was followed by staining with 3 µl of 2% uranyl acetate for 1 min and 30 s. After the stain was wicked away, grids were left to dry for ∼1–2 min. For imaging, a JEOL 1011 electron microscope was used to acquire 40 images from each grid where the microscopist was blinded to sample identities. After moving to the centre of a grid square at low magnification (×600), the magnification was adjusted to ×100 000 for image acquisition. After acquiring an image, the next image was taken on an adjacent grid square such that 40 unique grid squares were randomly sampled. The experimenter remained blinded to sample identity during quantification of fibrils. Fibrils were characterized and selected using PHF-resembling criteria: 10–20 nm in width and at least half a turn of the helical filament (> ∼35 nm) in length.

Results

We applied biochemical, mass spectrometry and functional assays to fully characterize the molecular features of HMW tau and to expand our understanding of the relationship between HMW and PHF tau isolated from Alzheimer's patients. The term high molecular weight 'HMW' refers to the property of these PBS extract tau species derived from Alzheimer's disease brain to elute from a size exclusion column in the early fractions. HMW tau is essentially not present in control brains. By contrast, low molecular weight (LMW) tau elutes substantially later and is abundantly present in both Alzheimer's disease and control brains. We specifically aimed to address five major questions: (i) What are the molecular features of HMW tau? (ii) How do those molecular features correlate with the seeding ability of HMW tau? (iii) What is the relationship between HMW and PHF tau in terms of PTMs? (iv) Is there heterogeneity among samples that is reflected in both HMW and PHF tau forms? and (v) Are there unique PTMs that correlate with bioactivity or clinical measures? Alzheimer's disease patients and healthy control post-mortem brain tissue homogenates were prepared and subjected to SEC to isolate early eluting HMW and late eluting LMW fractions. Tau present in these HMW and LMW fractions were

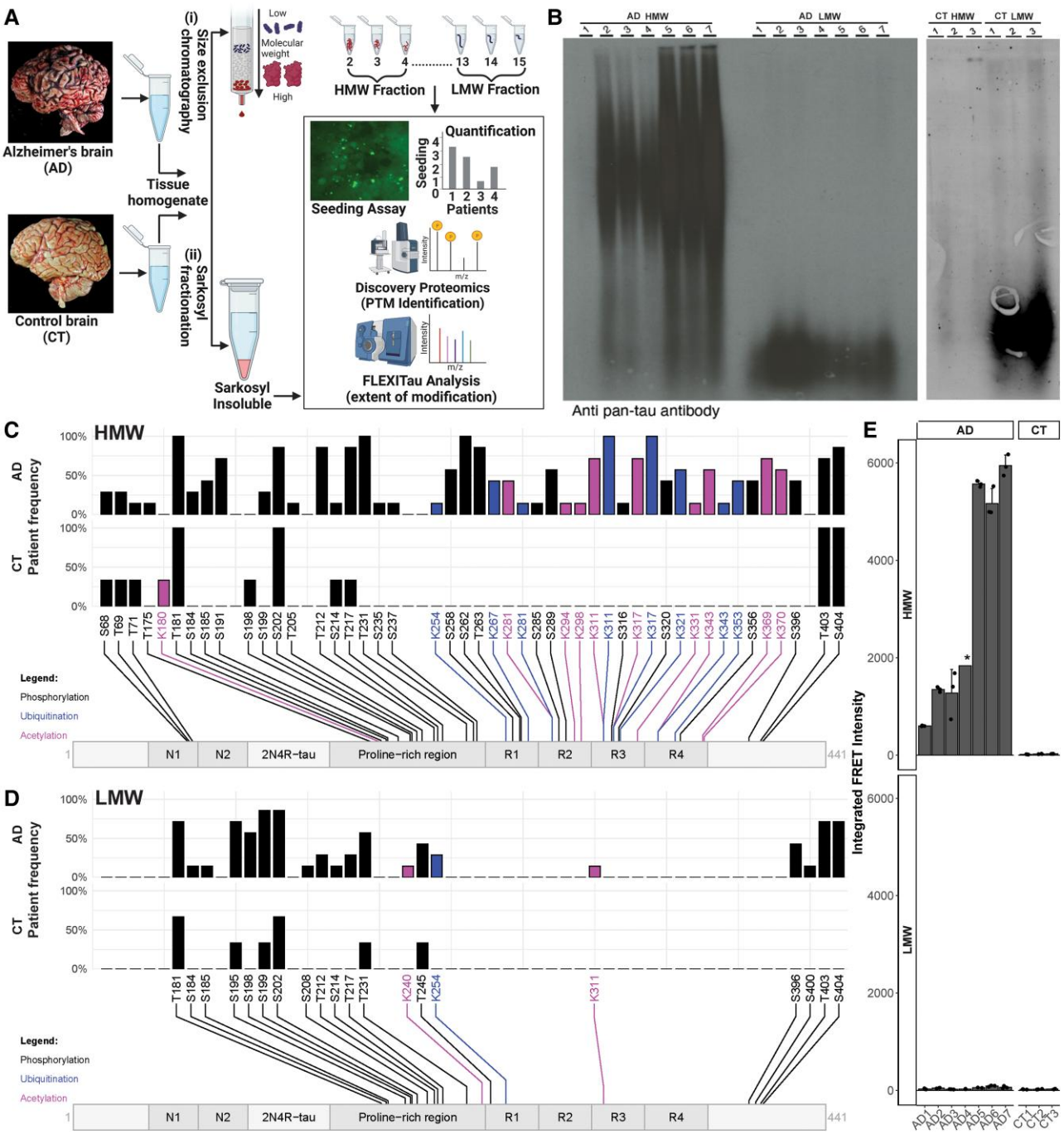

Figure 1 Preparation and characterization of HMW, LMW and PHF tau. (**A**) Schematic of workflow used in this study. Human Alzheimer's disease (AD) and control (CT) subjects brain tissue homogenate was used for (i) size exclusion chromatography (SEC); and (ii) for the sarkosyl enrichment method. SEC high molecular weight (HMW) and low molecular weight (LMW) fractions from Alzheimer's disease and control subjects were tested for seeding ability using biosensor cells. HMW and LMW fractions were further processed and analysed by mass spectrometry (MS) to identify the post-translational modification sites and to determine the extent of modification, respectively. Created using BioRender software. (**B**) Brain extracts from seven Alzheimer's disease and three control participants in our study were separated using a SEC column. HMW and LMW fractions were run on a semi-denaturing detergent agarose gel electrophoresis and revealed by a total tau antibody (Dako). (**C**) Post-translational modification (PTM) map of Alzheimer's disease and control HMW tau is shown. Position of the PTM is mapped on 2N4R tau isoform. (**D**) PTM of Alzheimer's disease and control LMW tau is shown. Position of the PTM is mapped on 2N4R tau isoform. (**E**) Using biosensor cell assay, seeding analysis for Alzheimer's disease and controls, HMW and LMW tau was performed.

compared to tau obtained from the same brain samples using a classical sarkosyl extraction for insoluble, fibrillar PHF tau. A schematic of the workflow used in this study is shown in Fig. 1A. The detailed demographics of the Alzheimer's disease and control subjects used in this study are provided in Supplementary Table 1.

Characterization of high and low molecular weight tau from Alzheimer's disease and control brain tissue

By SEC, the total protein extracted from Alzheimer's disease and control subjects' post-mortem brain tissue was separated into

HMW and LMW fractions (Fig. 1A). A representative SEC profile is shown in Supplementary Fig. 1. A calibration of the SEC column showed that the HMW tau is eluted after the void volume with molecules of molecular size of 600 kDa and lower, while the LMW tau is eluted, as expected, with molecules of molecular size <75 kDa (Supplementary Fig. 1). Fractions of HMW and LMW were run on a semi-denaturing detergent agarose gel electrophoresis and revealed by a total tau antibody (Fig. 1B). Prior to MS processing and analysis, the HMW fraction was ultra-centrifuged to concentrate the sample. Western blot and silver stain demonstrate that the vast majority of both tau bioactive seeds and total protein were pelleted (Supplementary Fig. 2). Moreover, representative transmission electron microscopy images of the pelleted material reveal primarily amorphous material, with occasional fibrils (Supplementary Fig. 3). By contrast, sarkosyl preparations contain, as expected, numerous PHFs (Supplementary Fig. 4). In addition, we evaluated the individual Fractions 2 to 4 and show that the PHF-like structures observed in the HMW fractions originate mostly from the first fraction and the fibril number decreases to nearly zero in the following fractions (Supplementary Fig. 5). Conversely, the seeding activity increases from Fractions 2 to 4, thus consistent with the hypothesis that seeding can be dissociated from the presence of fibrils (Supplementary Fig. 5). A more detailed biological comparison and quantitation of fibrils in HMW and sarkosyl tau transmission electron microscopy preparations can be found in Mate de Gerando *et al.*[34] These experiments support the idea that tau bioactive seeds were concentrated by ultra-centrifugation, without modifying the overall conformation.

HMW and LMW fractions isolated from each subject were further processed and analysed by MS. Using an MS-based discovery proteomics approach,[25,35] we identified a total of 45 PTMs on Alzheimer's disease HMW tau, including 28 phosphorylation, eight ubiquitination and nine acetylation sites on multiple residues (Fig. 1C). Amino acid sequence coverage of up to 90% of 2N4R tau protein was achieved; however, the majority of the PTM sites were present in the proline-rich region (PRR) and microtubule binding domain (MBD) region (Fig. 1C). Of 45 PTMs, modifications like phosphorylation at T181, S202, T212, T217, T231, S262, T263, T403 and S404; ubiquitination at K311, K317 and K321; acetylation at K311, K317, K343, K369 and K370 were detected in high frequency in patients compared to other modifications (Fig. 1C). In the control subjects, substantially less tau was detected in the HMW fraction and that tau shows only 11 modifications in total, including 10 phosphorylation and one low frequency acetylation. Only phosphorylation at T181, S202, T403 and S404 were present in >50% of patients (Fig. 1C). We next mapped the PTMs present on LMW tau isolated from same Alzheimer's disease and control subjects. In Alzheimer's disease LMW tau, 17 phosphorylation sites were detected and only 8/17 sites (T181, S195, S198, S199, S202, T231, T403 and S404) were observed in >50% of patients (Fig. 1D). Two acetylation sites, at K240 and K311, and one ubiquitination at K254 were detected in low frequency, in <25% and 50% of patients, respectively (Fig. 1D). In control LMW tau, six modifications (phosphorylation only) were detected (Fig. 1D).

Next, seeding analyses of HMW and LMW tau were performed (Fig. 1E). Matching for amount of tau added to the assay, Alzheimer's disease HMW tau shows extremely high seeding activity, 150-fold more seeding activity compared to control tau. Alzheimer's disease LMW tau shows significantly reduced (70-fold less) seeding activity compared to Alzheimer's disease HMW tau, but 2-fold more seeding activity compared to control LMW tau, suggesting that even the presence of low levels of Alzheimer's disease-related PTMs can impact conformation of tau enough to lead to templated misfolding, although at a comparatively low level. HMW tau isolated from different Alzheimer's disease patients showed differential seeding activity (up to 10-fold difference among subjects), whereas HMW tau from control subjects showed similar (<2-fold difference among subjects) low seeding activity across all subjects (Fig. 1E). The differential seeding activity of HMW tau reflects patient heterogeneity, an observation consistent with our previous studies from a different cohort of patients.[10] A comparison of the PTM profile of HMW and LMW tau for Alzheimer's disease and control subjects are shown in Supplementary Fig. 6A and B, respectively. In Alzheimer's disease, the seed competent HMW tau, compared to LMW tau, has a distinct PTM profile, particularly the exclusive presence of seven ubiquitination and nine acetylation sites in the MBD region (Supplementary Fig. 6A). In contrast to the differences observed between HMW and LMW tau in Alzheimer's disease, the PTM profile of control HMW and LMW tau is similar and only few modifications were observed, and only phosphorylation at T181 and S202 was identified in >50% of control patients in both HMW and LMW tau (Supplementary Fig. 6B). The detection of multiple modification sites uniquely in HMW tau isolated from Alzheimer's disease and not detected in either HMW tau from controls and LMW tau from Alzheimer's disease and controls, suggests the role of these unique modification's sites in the seeding activity of HMW tau.

Correlation between high molecular weight tau features and its seeding ability

Next, we asked whether the extent of tau PTMs on proteopathic HMW tau is associated with its seeding competency. We therefore quantified the seeding competency of HMW tau isolated from the seven Alzheimer's disease patients analysed in Fig. 1 and correlated it with the number of tau PTMs observed in each case. The amount of modified tau, as well as the total number of PTMs observed, correlate with tau seeding (Fig. 2A and B). The number of phosphorylation, ubiquitination and acetylation sites are each significantly associated with tau seeding competency (Fig. 2C–H, respectively) suggesting that the presence of these PTMs—i.e. negative charges of the phosphate groups or the neutralization of the lysine positive charges by acetylation and/or ubiquitination in the microtubule binding domain—contribute to, or correlate with, conformational changes required for seed competence and likely contribute to the properties of tau that lead it to elute in the HMW fraction from a size exclusion column. Immunodepletion using diverse antibodies targeted against phosphorylated tau is able to reduce seeding activity of the samples, although often to a limited extent.[10,26] The above analyses used as a denominator for seeding the amount of brain used in the preparation (seeding/wet weight). We found that the amount of tau in the HMW fraction correlates strongly with extent to which it is modified; as expected, the amount of bioactivity correlates with both amount and extent of modifications (Supplementary Fig. 7). In light of the presence of multiple ubiquitination sites on tau as identified by mass spectrometry (Fig. 1C), we hypothesize that ubiquitination, as an indirect marker of 'misfolded' proteins, correlates with the conformational changes that define seeding-competency of HMW tau. We performed a western blot experiment to show that tau and ubiquitin have the same migration pattern as separated by SDS PAGE and that tau is enriched in a ubiquitin immunoprecipitation

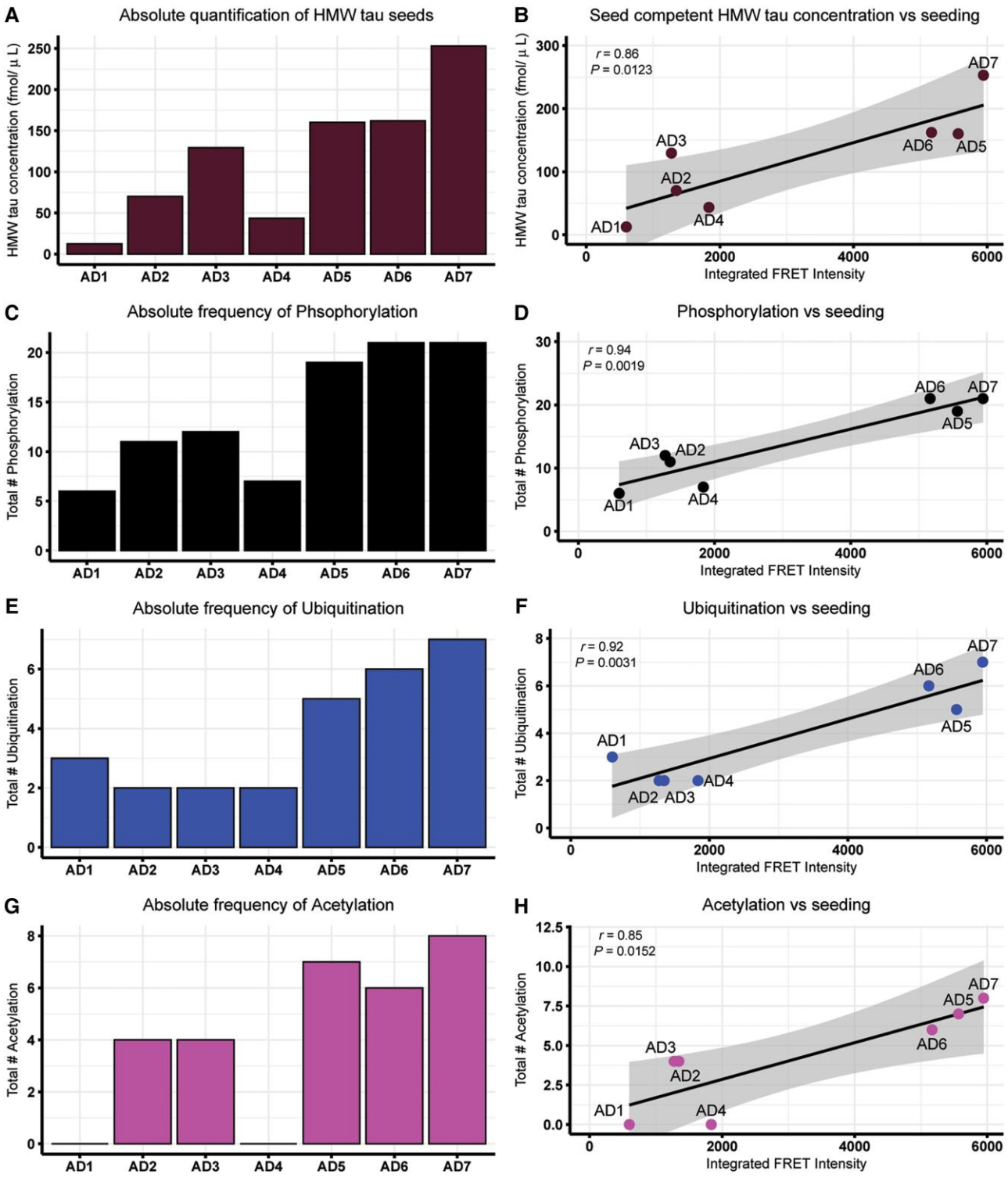

Figure 2 HMW seed competent tau PTMs correlate with seeding competency. (**A**) Absolute quantification of high molecular weight (HMW) seed competent tau concentration by the FLEXITau[24] mass spectrometry (MS) assay. $n = 7$ individual human participants. (**B**) Correlation between HMW seed competent tau absolute concentrations and tau seeding. (**C** and **D**) Associations between tau seeding and the number of phosphorylation sites, ubiquitination sites (**E** and **F**) or acetylation sites (**G** and **H**). Correlations were performed using a two-tailed Spearman's rank non-parametric test, and *P*- and *r*-values are indicated on each plot. FRET = fluorescence resonance energy transfer; PTM = post-translational modification.

(Fig. 3A–C). To further test the idea that ubiquitinated tau species correspond to those involved in seeding phenomena, we examined the seeding competency of HMW tau species immunodepleted with an anti-ubiquitin antibody. As hypothesized, immunoprecipitation of ubiquitin drastically reduced the amount of tau seeding in all the samples (Fig. 3D). This result confirms the MS data demonstrating that seed-competent HMW tau molecules are highly ubiquitinated.

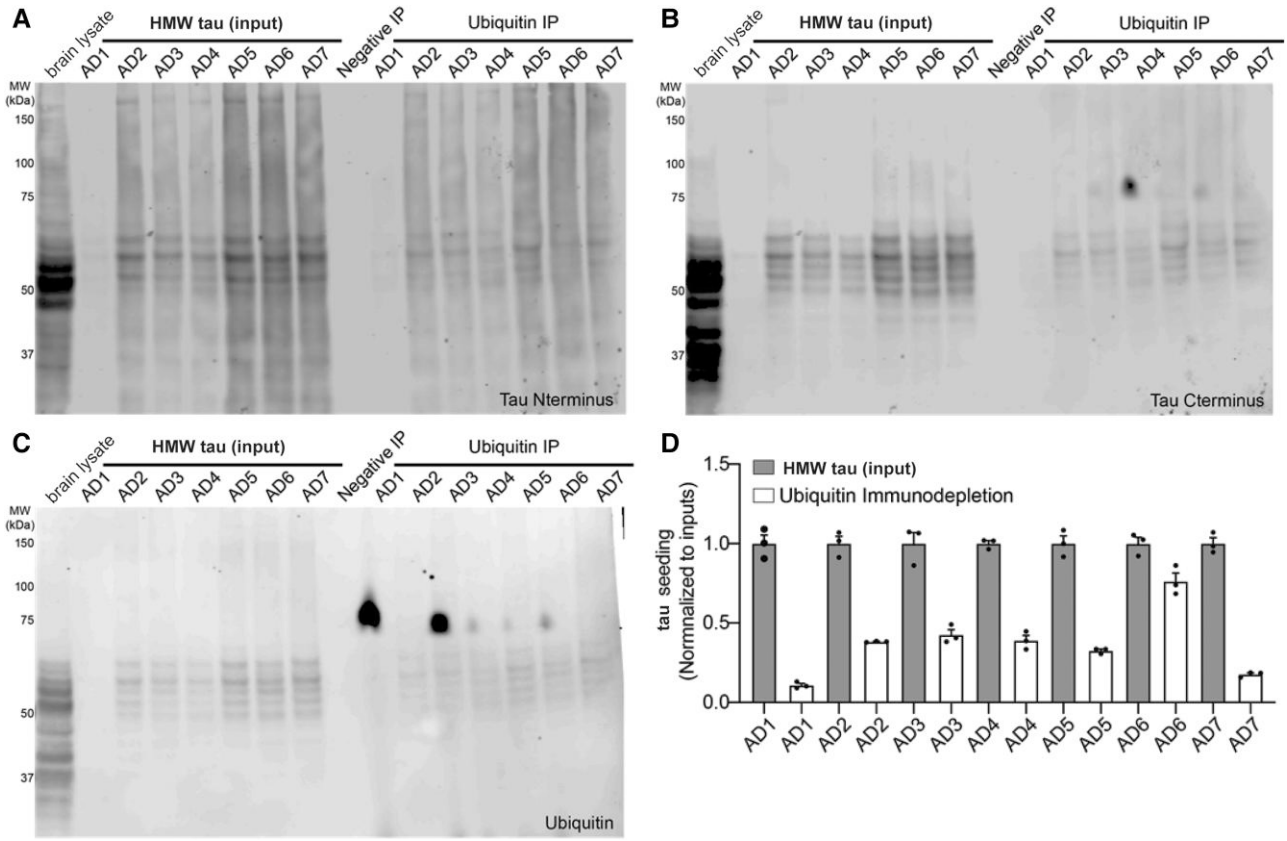

Figure 3 Proteopathic seed competent tau is ubiquitinated. (**A–C**) Tau extracted from the brain homogenate of seven different Alzheimer's disease (AD) cases as well as immunoprecipitated (IP) fractions using an anti-ubiquitin antibody were analysed by western blot using the following primary antibodies: N-terminal domain of tau (**A**), C-terminal domain of tau (**B**) and ubiquitin (**C**). (**D**) Tau was immunoprecipitated using an anti-ubiquitin antibody and the immunodepleted fractions were run on a seeding biosensor assay showing a high and reproducible reduction of tau seeding. Samples were normalized for the amount of tau present in the input. HMW = high molecular weight.

High molecular weight and paired helical filament tau isolated from Alzheimer's disease patients are similar, but distinct

To directly compare the molecular features of seed competent HMW tau to that of PHF tau, we employed the sarkosyl fractionation method and isolated insoluble PHF tau from the same Alzheimer's disease subjects (Fig. 1A and B). As shown in Supplementary Fig. 4 by transmission electron microscopy representative images, the sarkosyl fractionation method yield more fibrils than the HMW tau preparation. MS analysis revealed key similarities between HMW and PHF tau. High frequency PTMs like phosphorylation sites at T181, T217, T231, S235, S262, T263, S396, S400, T403, S404, ubiquitination sites at K311, K317 and acetylation sites at K317 and K369 were observed in sarkosyl insoluble PHF tau (Fig. 4A), consistent with a previously published report on a large Alzheimer's disease cohort.[22] These PTMs were also present in HMW tau (Fig. 4A). A direct comparison of all PTMs identified in HMW and PHF tau is shown in Fig. 4A.

A handful of sites were present predominantly in the HMW tau fraction, including a cluster near the N-terminus at positions S68, T69 and T71, T205 in the proline rich region, and acetylation/ubiquitination sites K281 and K294 in exon 10 (Fig. 4A). By contrast, the sarkosyl fraction had a substantially greater number of PTMs, scattered throughout the entire molecule (Fig. 4A), although the overlap of sites was essentially universal.

The second major observation is that there was clear heterogeneity in the exact sites present in each case, emphasizing heterogeneity among patients. We compared the PTMs detected in HMW and PHF tau extracted from patients with low (Patient AD1), medium (Patient AD3) and high (Patient AD7) aggregated tau amount (Fig. 4B–D, respectively). The PTM profile comparison of HMW and PHF for four other Alzheimer's disease subjects including Patients AD2, AD4, AD5 and AD6, are shown in Supplementary Fig. 8–D, respectively. This analysis shows that the patient heterogeneity is reflected in both HMW and PHF tau to the same extent and therefore HMW tau mirrored the patient's heterogeneity observed in PHF tau and may represent disease stage or individual differences in 'strain'. The presence of a minimum set of common modifications across subjects suggests that there is a core set of modifications associated with the specific conformation responsible for the templated misfolding of proteopathic seeds and ultimately PHFs, and yet there is considerable heterogeneity among individuals in this early pathological feature. Interestingly, ubiquitination and acetylation are exclusively detected in the microtubule binding domain, whereas phosphorylation is predominantly detected in the proline rich region.

We next compared the profile of each tau peptide from HMW and PHF tau analysed by FLEXITau assay (Fig. 4E). The FLEXITau quantification method[22,24] determines the extent of the post-translational modifications of all detected tau peptides from N- to C-terminus. The HMW and PHF FLEXITau profile looks very similar showing enrichment of the peptide ranging from amino acid 341–371 of the microtubule

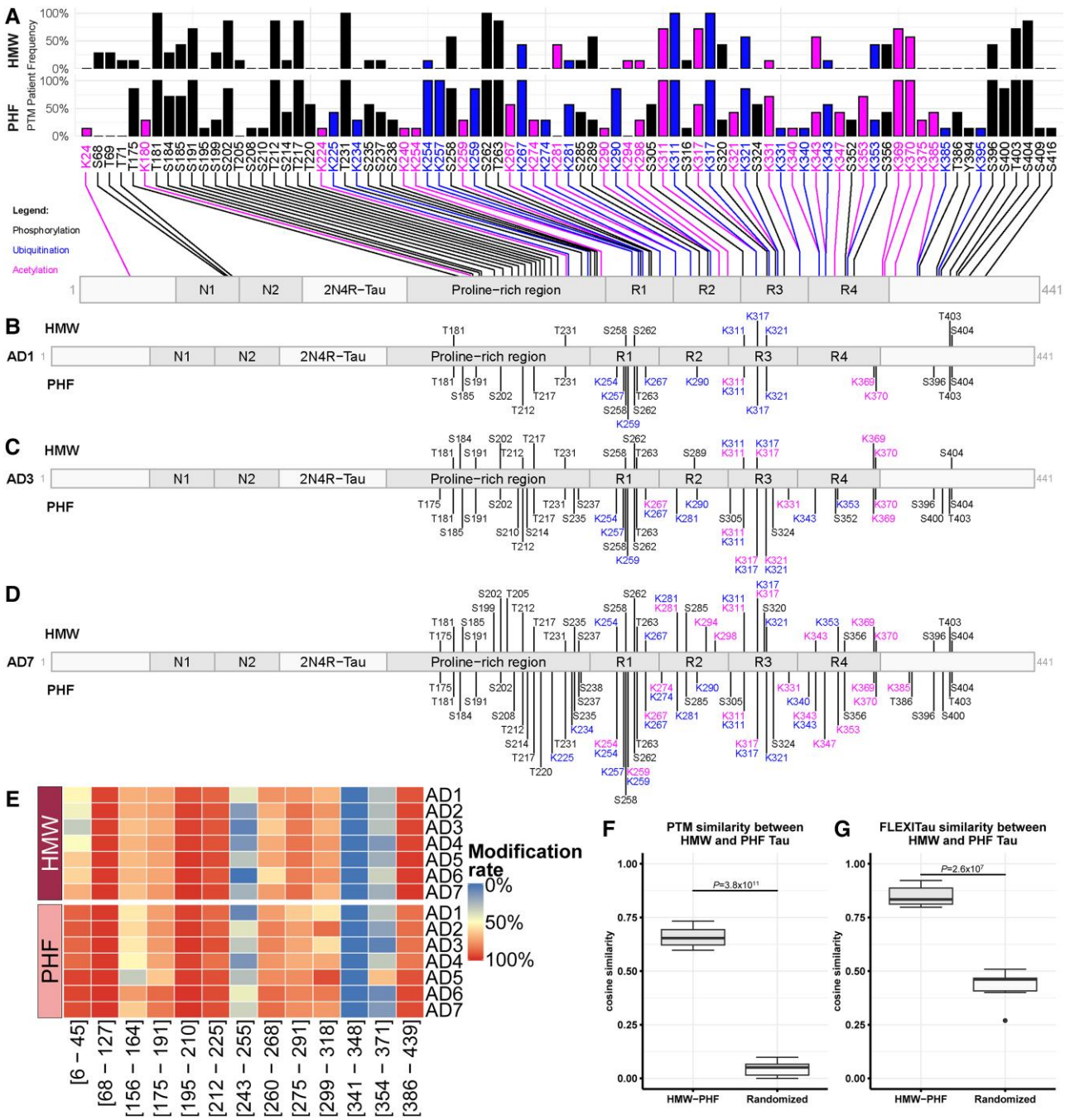

Figure 4 Similarities between HMW and PHF tau isolated from Alzheimer's disease patients. (**A**) Cumulative post-translational modifications (PTMs) map of high molecular weight (HMW) and sarkosyl insoluble (paired helical filaments, PHF) tau extracted from Alzheimer's disease (AD) brain tissue. The modification sites are schematically mapped on 2N4R tau from the N-terminal domain (amino acid 1) to the C-terminal domain (amino acid 441). Phosphorylation sites are indicated in black, ubiquitination sites in blue and acetylation sites in pink. (**B**–**D**) Examples of PTM maps of HMW and sarkosyl insoluble (PHF) tau extracted from Alzheimer's disease patients with low, medium and high tau load, respectively. (**E**) FLEXITau quantification heat map of HMW and sarkosyl insoluble (PHF) tau across all the subjects. The number e.g. [6–23], on the *y*-axis represents the position of the amino acids of the detected 2N4R tau peptides. The heat map shows the extent of modification of each peptide, red means highly modified and blue means less or no modification. (**F** and **G**) Shows the cosign similarity between HMW and sarkosyl insoluble (PHF) tau extracted from Alzheimer's disease brain tissue, based on PTM and FLEXITau quantification data, respectively.

binding region (Fig. 4E), also showing cleavage and/or modification of the C-terminal region ranging from amino acid 396 to 439 (Fig. 4E). To determine the relationship between the HMW and the PHF tau we performed a cosine similarity analysis by comparing the PTM sites and extent of modification for each tau peptide from FLEXITau analysis, for PBS proteopathic seeds with sarkosyl insoluble material in each of the seven samples. This analysis (in which a value of 1.0 is identity and a value of 0 is unrelated) showed a similarity of ~0.65 ($P = 7.3 \times 10^{-11}$) and ~0.85 ($P = 2.6 \times 10^{-9}$) for the HMW tau and the PHF tau based on PTM and FLEXITau data, respectively (Fig. 4F and G), compared to a random control. This shows both a very significant level of overlap but also highlights the non-identity of the sample populations.

Importantly, the overall cumulative number of PTMs is substantially less in the HMW fraction than observed in matched PHF samples. The PHF data in these samples mirrored closely the data obtained from our previous study of a large cohort of Alzheimer's disease patients.[22] A comparison of the PTM profile of HMW, LMW and PHF tau in this study and a previously published study by Wesseling *et al.*[22] is shown in Supplementary Fig. 9. While the patterns of PTMs observed in the current study are very similar to those we have reported in an earlier report with a smaller group of HMW and LMW samples,[22] there are some differences that might reflect differences in protein preparations, technique or in interindividual variations.

Discussion

Tau proteopathic material PBS extracted from human Alzheimer's disease brains is able to propagate tau pathology in the CNS,[10,15,16,20,27] with the ability to be taken up by neurons, escape to the cytoplasm and engage tau (and tau aggregation reporter molecules). Nonetheless, although they are presumed to be on pathway to tau fibrils, these proteopathic seeds have never been fully characterized and how such tau species compare to the end stage neuropathological feature, the PHFs of NFTs, has remained uncertain. We used MS and bioactivity assays to characterize these proteopathic seeds and learned that they closely resemble, but are distinct from, NFTs. While nearly all post-translational modifications on HMW tau are shared between HMW and PHF tau, only a small subset of PTMs present in the highly modified PHF fraction are found in the HMW tau. These modifications suggest that the minimum set of PTMs observed on HMW tau is sufficient to generate the conformational structure that underlies the seeding activity observed. Thus, despite very common characteristics, tau HMW proteopathic seeds differ from PHFs by their PTM content[22,23] arguing against the idea that HMW tau proteopathic seeds are simply broken up fragments of mature PHFs. Transmission electron microscopy of the HMW and sarkosyl preparations show primarily amorphous aggregates and infrequent short fibrils in the HMW samples, and extensive PHF in the sarkosyl preparations, confirming the biophysical differences that are reflected by the MS and bioactivity assays.

Our dataset reveals the presence of multiple ubiquitination modifications on tau present in both HMW proteopathic seeds and mature fibrils. While ubiquitination has been identified in mature tau fibrils,[22,23] we now also demonstrate their presence on proteopathic seed species. This would suggest that tau proteins are ubiquitinated early in their assembly process to form multimers, but, paradoxically, these species do not seem to undergo proteasome-mediated degradation. We speculate that early PTMs of sites around the microtubule binding region take place, contribute to stabilizing the tau structure in a pathogenic conformation, and to its multimerization. Multimerization may create a species that is likely not a good proteosome substrate, despite the presence of ubiquitin moieties.

Ubiquitination of tau appears to be important in determining structure of tau inclusions in the context of corticobasal degeneration,[28] leading to different strains. A recent study shows lysine 63-linked ubiquitination of tau oligomers contributes to the pathogenesis of Alzheimer's disease[29] and this study is consistent with the idea that ubiquitination influences formation, deposition and spreading of pathological tau oligomers and contributes to the Alzheimer's disease aetiology. While ubiquitination can result in the degradation of monomeric tau by the proteosome,[30,31] the current work suggests that ubiquitination may not always result in the clearance of oligomeric tau molecules. Taken together with these studies, our results suggest that ubiquitination of tau leads to stable conformers with potentially differential biological actions.

Recent elegant structural cryo-EM studies[32] document that a fragment consisting of amino acids 297–391 of recombinant tau, prepared without any post-translational modifications, was able to form a structure closely resembling the core fold of mature PHFs, yet extending the molecule on either the N- or C-terminal sides largely abrogated the ability to form the appropriate structure. Mature PHFs, as well as the oligomeric bioactive seed competent species we focus on here, extend beyond this 297–391 core and have some molecules of full-length tau with an unmodified N-terminus, while the C-terminal domain is highly phosphorylated or cleaved. Thus, we postulate that the presence of the post-translational modifications described herein provides insight to the structural alterations in tau that allow the multimerization drive of the core domain to overcome the endogenous resistance to multimerization encoded by the N- and C-terminal domains.

A recent study using modified tau constructs examining the sequential and interdependent nature of tau phosphorylation patterns in HEK cells identified several potential master sites for phosphorylation, including N-terminal sites T50 and T69 and sites T181 and T205 within the proline-rich domain.[36] In this context, the current results showing that HMW oligomeric species of tau derived from human brain are highly phosphorylated at pos T181, but not the other 'master sites' for sequential interdependent phosphorylation events, may focus attention on this site and the kinases, including p38α, that are known to phosphorylate it as an early event in Alzheimer's disease-related tau pathogenesis.

In summary, using MS we define the molecular features of the proteopathic seed competent HMW tau. We show that these tau seeds derived from human Alzheimer's disease brains are distinct from, but closely related to, PHFs. The results provide insight into key PTMs associated with a specific pathogenic conformation in the context of human disease and thus into the structural alterations that are key for the earliest steps of templated misfolding of tau aggregates. A future study aiming at determining the absolute amount of different PTMs per tau molecule would enable further understanding of the role of combinatorial or site-specific PTM on the bioactivity of tau molecules.

Data availability

All requests for raw and analysed data and materials are promptly reviewed by the Partners Healthcare innovation department to verify whether the request is subject to any intellectual property or confidentiality obligations. Patient-related data not included in the paper may be subject to patient confidentiality. Any data and materials that can be shared will be released via a Material Transfer Agreement upon reasonable request to the corresponding author. The mass spectrometry proteomics data have been deposited to the ProteomeXchange Consortium via the PRIDE [37] partner repository with the dataset identifiers PXD032192 and PXD036692.

Acknowledgements

We thank P. Dooley, J. A. Gonzalez and T. Connors for help with brain sampling and M. Diamond (UT Southwestern, Dallas, Texas) for the generous gift of the TauRD-P301S-CFP/YFP cells.

Funding

The work was supported by grants from the Tau Consortium of Rainwater Charitable Foundation (B.T.H. and J.S.), National

Institute of Health R56AG061196, RF1AG059789, RF1AG058674 and P30AG062421 (B.T.H.), the Alzheimer's Association [2018-AARF-591935 (S.D.)], the Martin L. and Sylvia Seevak Hoffman Fellowship for Alzheimer's Research (S.D.) and National Institute of Health/ National Institute of Neurological Disorders and Stroke U01 5U01NS110438-02 (J.S).

Competing interests

B.T.H. has a family member who works at Novartis and owns stock in Novartis; he serves on the SAB of Dewpoint and owns stock. He serves on a scientific advisory board or is a consultant for AbbVie, Aprinoia Therapeutics, Arvinas, Avrobio, Axial, Biogen, BMS, Cure Alz Fund, Cell Signaling, Eisai, Genentech, Ionis, Novartis, Sangamo, Sanofi, Takeda, the US Dept of Justice, Vigil, Voyager. His laboratory is supported by research grants from the National Institutes of Health, Cure Alzheimer's Fund, Tau Consortium, and the JPB Foundation—and sponsored research agreements from AbbVie, and BMS.

Supplementary material

Supplementary material is available at *Brain* online.

References

1. Goedert M. Tau filaments in neurodegenerative diseases. *FEBS Lett*. 2018;592:2383-2391.
2. Jicha GA, Bowser R, Kazam IG, Davies P. Alz-50 and MC-1, a new monoclonal antibody raised to paired helical filaments, recognize conformational epitopes on recombinant tau. *J Neurosci Res*. 1997;48:128-132.
3. Mandelkow E, von Bergen M, Biernat J, Mandelkow EM. Structural principles of tau and the paired helical filaments of Alzheimer's disease. *Brain Pathol*. 2007;17:83-90.
4. Fitzpatrick AWP, Falcon B, He S, *et al*. Cryo-EM structures of tau filaments from Alzheimer's disease. *Nature*. 2017;547:185-190.
5. Falcon B, Zhang W, Murzin AG, *et al*. Structures of filaments from Pick's disease reveal a novel tau protein fold. *Nature*. 2018;561:137-140.
6. Falcon B, Zhang W, Schweighauser M, *et al*. Tau filaments from multiple cases of sporadic and inherited Alzheimer's disease adopt a common fold. *Acta Neuropathol*. 2018;136:699-708.
7. Falcon B, Zivanov J, Zhang W, *et al*. Novel tau filament fold in chronic traumatic encephalopathy encloses hydrophobic molecules. *Nature*. 2019;568:420-423.
8. Zhang W, Tarutani A, Newell KL, *et al*. Novel tau filament fold in corticobasal degeneration. *Nature*. 2020;580:283-287.
9. Shi Y, Zhang W, Yang Y, *et al*. Structure-based classification of tauopathies. *Nature*. 2021;598:359-363.
10. Dujardin S, Commins C, Lathuiliere A, *et al*. Tau molecular diversity contributes to clinical heterogeneity in Alzheimer's disease. *Nat Med*. 2020;26:1256-1263.
11. Sepulveda-Falla D, Chavez-Gutierrez L, Portelius E, *et al*. A multifactorial model of pathology for age of onset heterogeneity in familial Alzheimer's disease. *Acta Neuropathol*. 2021;141:217-233.
12. Jackson SJ, Kerridge C, Cooper J, *et al*. Short fibrils constitute the Major Species of seed-competent tau in the brains of mice transgenic for human P301S tau. *J Neurosci*. 2016;36:762-772.
13. Kopeikina KJ, Hyman BT, Spires-Jones TL. Soluble forms of tau are toxic in Alzheimer's disease. *Transl Neurosci*. 2012;3:223-233.
14. Mirbaha H, Holmes BB, Sanders DW, Bieschke J, Diamond MI. Tau trimers are the minimal propagation unit spontaneously internalized to seed intracellular aggregation. *J Biol Chem*. 2015;290:14893-14903.
15. Takeda S, Wegmann S, Cho H, *et al*. Neuronal uptake and propagation of a rare phosphorylated high-molecular-weight tau derived from Alzheimer's disease brain. *Nat Commun*. 2015;6:8490.
16. Usenovic M, Niroomand S, Drolet RE, *et al*. Internalized tau oligomers cause neurodegeneration by inducing accumulation of pathogenic tau in human neurons derived from induced pluripotent stem cells. *J Neurosci*. 2015;35:14234-14250.
17. Maeda S, Sahara N, Saito Y, *et al*. Granular tau oligomers as intermediates of tau filaments. *Biochemistry*. 2007;46:3856-3861.
18. Maeda S, Sahara N, Saito Y, Murayama S, Ikai A, Takashima A. Increased levels of granular tau oligomers: An early sign of brain aging and Alzheimer's disease. *Neurosci Res*. 2006;54:197-201.
19. Sahara N, DeTure M, Ren Y, *et al*. Characteristics of TBS-extractable hyperphosphorylated tau species: Aggregation intermediates in rTg4510 mouse brain. *J Alzheimers Dis*. 2013;33:249-263.
20. Lasagna-Reeves CA, Castillo-Carranza DL, Sengupta U, *et al*. Alzheimer brain-derived tau oligomers propagate pathology from endogenous tau. *Sci Rep*. 2012;2:700.
21. Lasagna-Reeves CA, Castillo-Carranza DL, Sengupta U, *et al*. Identification of oligomers at early stages of tau aggregation in Alzheimer's disease. *FASEB J*. 2012;26:1946-1959.
22. Wesseling H, Mair W, Kumar M, *et al*. Tau PTM profiles identify patient heterogeneity and stages of Alzheimer's disease. *Cell*. 2020;183:1699-1713.e13.
23. Arakhamia T, Lee CE, Carlomagno Y, *et al*. Posttranslational modifications mediate the structural diversity of tauopathy strains. *Cell*. 2020;180:633-644.e12.
24. Mair W, Muntel J, Tepper K, *et al*. FLEXITau: Quantifying post-translational modifications of tau protein in vitro and in human disease. *Anal Chem*. 2016;88:3704-3714.
25. Zhang Y, Fonslow BR, Shan B, Baek MC, Yates JR III. Protein analysis by shotgun/bottom-up proteomics. *Chem Rev*. 2013;113:2343-2394.
26. Nobuhara CK, DeVos SL, Commins C, *et al*. Tau antibody targeting pathological species blocks neuronal uptake and interneuron propagation of tau in vitro. *Am J Pathol*. 2017;187:1399-1412.
27. Wu JW, Herman M, Liu L, *et al*. Small misfolded tau species are internalized via bulk endocytosis and anterogradely and retrogradely transported in neurons. *J Biol Chem*. 2013;288:1856-1870.
28. Arakhamia T, Lee CE, Carlomagno Y, *et al*. Posttranslational modifications mediate the structural diversity of tauopathy strains. *Cell*. 2021;184:6207-6210.
29. Puangmalai N, Sengupta U, Bhatt N, *et al*. Lysine 63-linked ubiquitination of tau oligomers contributes to the pathogenesis of Alzheimer's disease. *J Biol Chem*. 2022;298:101766.
30. Dickey CA, Koren J, Zhang YJ, *et al*. Akt and CHIP coregulate tau degradation through coordinated interactions. *Proc Natl Acad Sci U S A*. 2008;105:3622-3627.
31. Ravalin M, Theofilas P, Basu K, *et al*. Specificity for latent C termini links the E3 ubiquitin ligase CHIP to caspases. *Nat Chem Biol*. 2019;15:786-794.
32. Lovestam S, Koh FA, van Knippenberg B, *et al*. Assembly of recombinant tau into filaments identical to those of Alzheimer's disease and chronic traumatic encephalopathy. *Elife*. 2022;11:e76494.
33. Maclean B, Tomazela DM, Shulman N, *et al*. Skyline: An open source document editor for creating and analyzing targeted proteomics experiments. *Bioinformatics*. 2010;26(7):966-968.

34. Mate De Gerando A, Welikovitch LA, Khasnavis A, *et al*. Tau seeding and spreading in vivo is supported by both AD-derived fibrillar and oligomeric tau. *Acta Neuropathol*. 2023; 146:191-210.
35. Aebersold R, Mann M. Mass spectrometry-based proteomics. *Nature*. 2003;422:198-207.
36. Stefanoska K, Gajwani M, Tan ARP, *et al*. Alzheimer's disease: Ablating single master site abolishes tau hyperphosphorylation. *Sci Adv*. 2022;8:eabl8809.
37. Perez-Riverol Y, Bai J, Bandla C, *et al*. The PRIDE database resources in 2022: A hub for mass spectrometry-based proteomics evidences. *Nucleic Acids Res*. 2022;50(D1):D543-D552.